

Table 1 Values of  $I_1$ ,  $I_2$ , and  $C_D$ <sup>a</sup>

	$x/d$	$I_1$	$I_2$	$C_D$
Present experiment $d = 12.5$ mm $R_d \approx 5600$	5	0.671	0.189	0.860
	10	0.728	0.122	0.850
	20	0.821	0.043	0.864
	30	0.891	0.005	0.896
	40	0.889	-0.007	0.882
	50	0.907	-0.009	0.898
	60	0.898	-0.010	0.888
Cantwell and Coles <sup>b</sup> : $R_d = 1200$ $R_d = 2000$ $R_d = 5000$				0.960
				0.820
				0.910
Data of Browne et al. <sup>1</sup> : $d = 2.67$ mm $R_d \approx 1200$	420	0.973	-0.003	0.97

<sup>a</sup>Errors in the estimate of  $I_1$  and  $I_2$  are of the order  $\pm 2\%$ .

<sup>b</sup>Values of  $C_D$  were obtained by drawing a mean curve through the data of several investigators (Fig. 1 of Cantwell and Coles<sup>8</sup>).

where  $p_1$  is the kinematic freestream static pressure. The use of Eq. (5) to determine the correct value of  $C_D$  does not account for the contribution of  $\bar{u}^2$  which may not be small. Taylor<sup>6</sup> pointed out that the error in the expression for  $C_D$ , obtained by Betz<sup>4</sup> and Jones<sup>5</sup> via a control-volume analysis without explicitly accounting for the normal stresses, may be small. The results presented in the next section indicate that the contribution from the normal stresses can be significant at small  $x/d$ .

Measurements close to the cylinder indicate that  $\bar{v}^2 > \bar{u}^2$ , possibly due to the vortex shedding and the relatively intense crossflow mixing associated with the motion induced by the vortices. As  $x/d$  increases, both  $\bar{u}^2$  and  $\bar{v}^2$  decrease, but in the far wake  $\bar{u}^2$  becomes larger than  $\bar{v}^2$ . This indicates that at some downstream location, the contribution from the normal stresses is zero (i.e.,  $I_2 = 0$ ) and an accurate value of  $C_D$  can be obtained from only a mean velocity profile at that location. Our aim was also to determine this location and estimate  $C_D$  as accurately as possible.

### Results

Measurements were made in the wake of a cylinder, over the range  $0 < x/d < 60$ , of diameter  $d = 12.5$  mm. A constant free-stream velocity  $U_1$  of 6.7 m/s was used and the corresponding Reynolds number  $R_d = U_1 d / \nu$  was 5600. At each  $x/d$  location, profiles of  $\bar{U}$ ,  $\bar{u}^2$ , and  $\bar{v}^2$  were determined by traversing an  $X$ -probe across the wake. The integrals  $I_1$  and  $I_2$  were estimated from these profiles. Table 1 summarizes the results obtained in the present experiments. At  $x/d = 30$ ,  $I_2$  is nearly zero, indicating that the contribution to  $C_D$  from the normal stresses at this location is negligible. For  $x/d > 30$ ,  $I_2$  changes sign but its magnitude is quite small. At  $x/d = 5$ ,  $I_2$  contributes 22% to  $C_D$  and the contribution decreases as  $x/d$  increases. At  $x/d = 20$ ,  $I_2$  contributes only 5% to the value of  $C_D$ . For  $x/d > 30$ , the contribution of  $I_2$  is negative, but negligible. A value of  $C_D$ , estimated for the far wake data of Browne et al.<sup>7</sup> is also shown in Table 1.

Values of  $C_D$  given in Table 1 are in reasonable agreement with available results in the literature (e.g., Cantwell and Coles<sup>8</sup>). Table 1 also indicates that for  $x/d \geq 30$ ,  $C_D$  is nearly constant. Allowing for the experimental uncertainty, the minimum distance at which the mean velocity profile can be used to determine  $C_D$  without correcting for the Reynolds-normal-stress term appears to be  $30d$ . This distance should be sufficiently large to allow any local freestream pressure disturbance, arising from the insertion of the cylinder in the (finite area) working section, to disappear. The minimum distance may depend on initial conditions (such as the nature of the

cylinder surface or the freestream turbulence) and the Reynolds number. It should be finally noted that the present estimate for this distance applies strictly to the flow behind a circular cylinder. When the wake-generating body is streamlined, or partially streamlined, the available  $u^2$  and  $v^2$  data, e.g., the measurements of Chevray and Kovasznay<sup>9</sup> for the wake of a thin flat plate or Chevray<sup>10</sup> for the wake of a six-to-one spheroid suggest that  $I_2$  does not change sign in these flows.

### References

- <sup>1</sup>Townsend, A. A., *The Structure of Turbulent Shear Flow*, Cambridge University Press, Cambridge, MA, 1956, Chap. 7.
- <sup>2</sup>Tennekes, H., and Lumley, J. L., *A First Course in Turbulence*, MIT Press, Cambridge, MA, 1972, Chap. 4.
- <sup>3</sup>Schlichting, H., *Boundary-Layer Theory*, 7th ed., McGraw-Hill, New York, 1969, Chap. 25.
- <sup>4</sup>Betz, A., "Ein Verfahren zur direkten Ermittlung des Profilwiderstandes," *Zeitschrift Flugtechnischer Motorluftschiffe*, Vol. 16, 1925, p. 42.
- <sup>5</sup>Jones, B. M., "The Measurement of Profile Drag by the Pitot Traverse Method," Aeronautical Research Council R&M 1688, 1936.
- <sup>6</sup>Taylor, G. I., "The Determination of Drag by the Pitot Traverse Method," Aeronautical Research Council R&M 1808, 1937.
- <sup>7</sup>Browne, L. W. B., Antonia, R. A., and Shah, D. A., "Turbulent Energy Dissipation in a Wake," *Journal of Fluid Mechanics*, Vol. 179, June 1987, pp. 307-326.
- <sup>8</sup>Cantwell, B., and Coles, D., "An Experimental Study of Entrainment of Transport in the Turbulent Near Wake of a Circular Cylinder," *Journal of Fluid Mechanics*, Vol. 136, Nov. 1983, pp. 321-374.
- <sup>9</sup>Chevray, R., and Kovasznay, L. S. G., "Turbulence Measurements in the Wake of a Thin Flat Plate," *AIAA Journal*, Vol. 7, Aug. 1969, pp. 1641-1643.
- <sup>10</sup>Chevray, R., "The Turbulent Wake of a Body of Revolution," *Journal of Basic Engineering*, Vol. 90, June 1968, pp. 275-284.

## Prediction of Inviscid Stagnation Pressure Losses in Supersonic Inlet Flows

David J. Azevedo,\* Ching Shi Liu,† and William J. Rae‡  
University at Buffalo,  
Buffalo, New York 14260

TO achieve a desired mass flow rate through a high-speed inlet, the stagnation pressure must be above some critical value. Stagnation, or total, pressure losses in bounded supersonic flows, such as those in a supersonic inlet, can result in the flow becoming unchoked (i.e., subsonic). It is important, therefore, to be able to predict these pressure drops if one is to produce a viable inlet design. The primary intention of this Note is to quantify the stagnation pressure losses associated with shock-wave systems that may be present in such high Mach number flows.

Figure 1, from Goldberg and Hefner,<sup>1</sup> is a graph of the maximum contraction ratio that can be achieved by a two-dimensional inlet and still be able to pass the intercepted mass

Received May 19, 1989; revision received Dec. 11, 1989; accepted for publication Dec. 29, 1989.

\*Visiting Lecturer, Department of Mechanical and Aerospace Engineering; currently Senior Engineer with United Technologies/Pratt and Whitney, West Palm Beach, FL. Member AIAA.

†Associate Professor, Department of Mechanical and Aerospace Engineering.

‡Professor, Department of Mechanical and Aerospace Engineering. Associate Fellow AIAA.

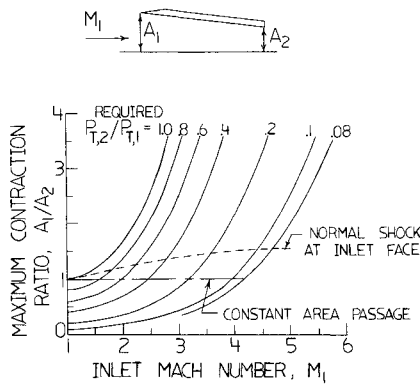


Fig. 1 Parameters governing the starting of supersonic and hypersonic diffusers (after Goldberg and Hefner<sup>1</sup>).

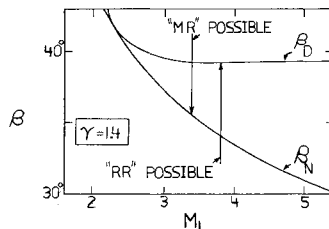
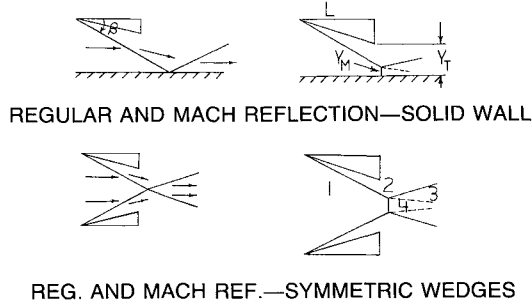


Fig. 2 Shock patterns that are observed in high-speed, steady flows (after Hornung and Robinson<sup>5</sup>).

inlet  $P_{t,2}/P_{t,1}$  as a parameter. The equation from which this graph is developed is<sup>2</sup>

$$(A_1/A_2)_{\max} = A_1/A_{2*} = \frac{1}{M_1} \left\{ \frac{1 + \frac{\gamma-1}{2} M_1^2}{\frac{\gamma+1}{2}} \right\}^{\frac{\gamma+1}{2(\gamma-1)}} \times (P_{t,2}/P_{t,1}) \quad (1)$$

where  $A_{2*}$  denotes sonic conditions at the downstream end. This relation is based on a one-dimensional flow approximation.

One difficulty with using this graph for practical inlet design is the specification of  $P_{t,2}/P_{t,1}$  solely from given freestream conditions. Stagnation pressure losses in these situations are normally associated with viscous effects such as boundary-layer growth and separation and are sometimes complicated by the presence of entropy layers. However, there are also losses associated with the presence of any shock-wave systems embedded within the duct, and it is of interest to be able to assess their importance even in the absence of boundary layers. Estimates of the losses attributable to these shocks can be made for the limiting cases of purely oblique waves inside the duct or a normal shock at the duct entrance; the present Note contains further results for intermediate cases where Mach reflection introduces a more complex wave system (see Fig. 2).

The three-shock system that characterizes Mach reflection can be caused by too large an inlet wedge angle  $\theta$  or an imposed high downstream pressure.<sup>3</sup> The phenomenon has been investigated both analytically<sup>4</sup> and experimentally<sup>5</sup> for the two-dimensional steady-flow situation; the interest has been primarily to determine the wedge angle causing transition from regular reflection (RR) to Mach reflection (MR), a transition illustrated in Fig. 2. In this figure,  $\beta$  represents the incident shock angle and is associated with the wedge angle  $\theta$ . The angle  $\beta_N$  is usually referred to as the "Von Neumann angle" and represents the minimum incident shock angle corresponding to transition from RR to MR. The angle  $\beta_D$  is that incident shock angle that results in a reflected shock angle equal to that associated (via oblique-shock relations) with detachment from a wedge. Thus, the figure indicates that the reflected wave "detaches" from the surface (or centerline, for a symmetric wedge arrangement) at an angle  $\beta_N$  which is less than that predicted by oblique-shock relations. An equation that illustrates how one may compute  $\beta_N$  from upstream conditions is provided in Ref. 13, p. 341 as well as in Refs. 4 and 6.

A recent study was conducted<sup>6</sup> to determine whether the Mach reflection patterns, and more specifically the normal shock length  $y_M$  shown in Fig. 2, could be predicted analytically given only the upstream flow conditions and wedge geometry. A complicating factor in simply applying the Rankine-Hugoniot equations to find the flow conditions in the uniform regions 1, 2, and 3 as well as the local shock angles is the nonuniform accelerating flow behind the normal shock wave. The acceleration is caused by the inclined slipstream that separates the supersonic flow in region 3 from the subsonic flow in region 4. The slipstream arises from the entropy difference in regions 3 and 4 and can be modeled as a vortex sheet<sup>7,8</sup> in the inviscid case and as a growing shear layer<sup>9</sup> in the viscous case. In Ref. 6, an isentropic one-dimensional flow model was used for the subsonic region; the slipstream was treated as a thin, straight discontinuity across which there was no mass flux. Other investigators<sup>10,11</sup> have found this one-dimensional approximation to be reasonable for similar situations. Viscous growth of the slipstream was determined by one of the authors<sup>6</sup> to be negligible for the test conditions considered in the present study.

Details of the approach used to determine the scale of the Mach reflection patterns are provided elsewhere.<sup>6</sup> Once the shock configuration is known, a mass-weighted value for the overall stagnation pressure drop in the duct may be developed. The weighting is needed to account for the fact that a portion

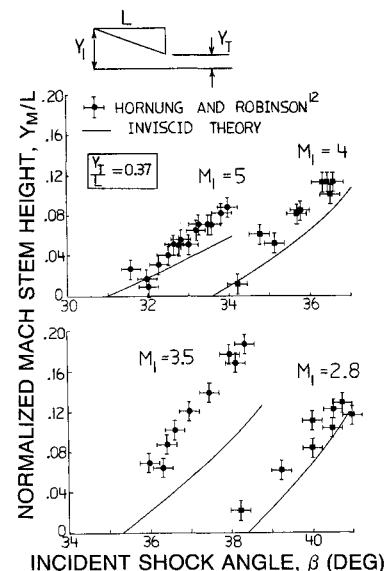


Fig. 3 Comparison of Mach stem height predictions and experimental data.

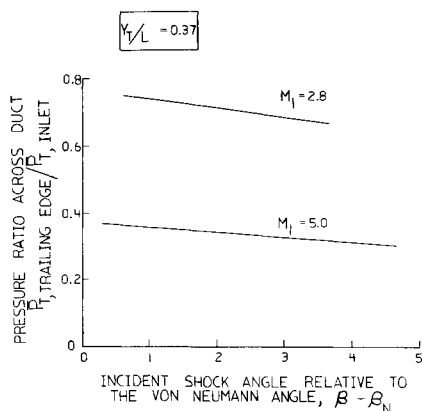


Fig. 4 Mass-averaged stagnation-pressure ratios developed from the predictions in Fig. 3.

of the duct flow is processed by oblique shocks, whereas the remainder encounters a normal shock wave.

One of the advantages of estimating the stagnation pressure losses due only to the flow across shocks is that experimental measurements of the overall  $P_t$  drop (which normally include viscous and inviscid contributions) can be better understood. This may help in the design of inlets of hypersonic flow situations where the source of the viscous contribution is difficult to evaluate. (Of course, the shock exists due to the action of viscous forces, but for our purposes the stagnation pressure drop across the shocks can be considered as an inviscid contribution to the overall stagnation loss in the duct.) In addition, if the shock-related contribution turns out to be much larger than that attributable to viscous effects, the designer could introduce methods for minimizing the scale of the shock system (in particular the size of the normal shock) since the largest  $P_t$  drops occur there.

As an example, Fig. 3 illustrates the predicted stem heights for freestream Mach numbers of 2.8 and 5.0, and comparison is made with certain unpublished data of Hornung and Robinson.<sup>12</sup> Figure 4 is a graph of the resultant  $P_t$  ratio across the duct as a function of the shock-angle difference  $\beta - \beta_N$ .

The wedge angles corresponding to the incident shock angles shown in Fig. 3 may be rather large for practical hypersonic diffusers. However, the angles shown may be approached during vehicle maneuvering or other transients, and thus the estimates described here may then apply.

### Acknowledgments

This work was supported by the NASA Office of Aeronautics and Space Technology under the Hypersonic Training and Research Program, Grant NAGW 966.

### References

- Goldberg, T. J., and Hefner J. N., "Starting Phenomena for Hypersonic Inlets with Thick Turbulent Boundary Layers at Mach 6," NASA TN D-6180, 1971.
- Zucrow, M. J., and Hoffmann, J. D., *Gas Dynamics*, Vol. 1, Wiley, New York, 1976.
- Henderson, L. F., and Lozzi, A., "Further Experiments on Transition to Mach Reflexion," *Journal of Fluid Mechanics*, Vol. 94, Pt. 3, 1979, pp. 541-559.
- von Neumann, J., "Oblique Reflection of Shocks," Navy Department (Bureau of Ordnance), Washington, DC, *Explosives Research Rept.* No. 12, 1943; see also *Collected Works*, Vol. 6, Pergamon, Oxford, 1963, pp. 238-299.
- Hornung, H. G., and Robinson, M. L., "Transition from Regular to Mach Reflection of Shock Waves, Part 2: The Steady-Flow Criterion," *Journal of Fluid Mechanics*, Vol. 123, 1982, pp. 155-164.
- Azevedo, D. J., "Prediction of Length Scales in a Mach Reflection Flowfield," Ph.D. Thesis, SUNY, Dept. of Mechanical and Aerospace Engineering, Univ. at Buffalo, May 1989.

<sup>7</sup>Henderson, L. F., "On the Confluence of Three Shock Waves in a Perfect Gas," *The Aeronautical Quarterly*, Vol. XV, May 1964, pp. 181-197.

<sup>8</sup>Hornung, H. G., "Regular and Mach Reflection of Shock Waves," *Annual Review of Fluid Mechanics*, Vol. 18, 1987, pp. 33-58.

<sup>9</sup>Ben-Dor, G., "A Reconsideration of the Three-Shock Theory for a Pseudo-Steady Mach Reflection," *Journal of Fluid Mechanics*, Vol. 181, 1987, pp. 467-484.

<sup>10</sup>Back, L. H., and Cuffel, R. F., "Viscous Slipstream Flow Downstream of a Centerline Mach Reflection," *AIAA Journal*, Vol. 9, No. 10, 1971, pp. 2107-2109.

<sup>11</sup>Chow, W. L., and Addy, A. L., "Interaction Between Primary and Secondary Streams of Supersonic Ejector Systems and Their Performance Characteristics," *AIAA Journal*, Vol. 2, No. 4, 1964, pp. 686-695.

<sup>12</sup>Hornung, H. G., personal communication, Graduate Aeronautics Laboratories, California Institute of Technology, 1988.

<sup>13</sup>Courant, R., and Friedrichs, K. O., *Supersonic Flow and Shock Waves*, Vol. 21, *Applied Mathematical Sciences Series*, Springer-Verlag, New York, pp. 340-341.

## Transonic Computations on a Natural Grid

R. K. Naeem\* and R. M. Barron†

University of Windsor, Windsor, Ontario, Canada

### Introduction

IN an earlier paper,<sup>1</sup> the authors have shown that the von Mises transformation provides a convenient computational domain for the finite difference solution of transonic full-potential flows. The resulting natural grid system consists of the streamlines  $\Psi = \text{const}$  and the Cartesian coordinate lines  $x = \text{const}$ , where  $\Psi(x, y)$  is the stream function. In this  $(x, \Psi)$  system, the computational domain is rectangular, and the coordinate curves  $\Psi = \text{const}$  are "body-fitting," thus eliminating the need to develop a body-conforming grid system using numerical grid generation techniques. It can be shown that transonic full-potential flow is governed by<sup>1</sup>

$$y_{\Psi}^2 y_{xx} - 2y_x y_{\Psi} y_{x\Psi} + (1 + y_x^2) y_{\Psi\Psi} = \frac{y_x y_{\Psi}^2 \rho_x}{\rho} - \frac{y_{\Psi} (1 + y_x^2) \rho_{\Psi}}{\rho} \quad (1)$$

$$\rho = \left[ 1 - \frac{(\gamma - 1) M_{\infty}^2}{2} \left( \frac{1 + y_x^2}{\rho^2 y_{\Psi}^2} - 1 \right) \right] \frac{1}{\gamma - 1} \quad (2)$$

where  $y = y(x, \Psi)$  is the equation defining the von Mises transformation and  $\rho$  is the density. Equation (1) may be viewed as a grid generation equation, but actually it represents the physical condition of irrotationality. This equation is solved for the geometrical unknown  $y(x, \Psi)$ , and hence we may consider Eq.(1) as tying together the flow geometry and the flow physics. The pressure coefficient is related to  $\rho$  by

$$C_p = \frac{2(\rho^{\gamma} - 1)}{\gamma M_{\infty}^2} \quad (3)$$

Received May 8, 1989; revision received Nov. 9, 1989. Copyright © 1990 by the American Institute of Aeronautics and Astronautics, Inc. All rights reserved.

\*Graduate Student, Department of Mathematics and Statistics.

†Professor, Department of Mathematics and Statistics; Director, Fluid Dynamics Research Institute.